Biosensors and Bioelectronics 33 (2012) 304–308

Contents lists available at SciVerse ScienceDirect

Biosensors and Bioelectronics

journal homepage: www.elsevier.com/locate/bios

Short communication

Electrical detection of biomolecular adsorption on sprayed graphene sheets

Tamon R. Page[a], Yuhei Hayamizu[a,b], Christopher R. So[a], Mehmet Sarikaya[a,*]

[a] Genetically Engineered Materials Science and Engineering Center, MSE, University of Washington, Seattle, WA 98195, USA
[b] PRESTO, Japan Science and Technology Agency (JST), 4-1-8 Honcho, Kawaguchi, Saitama 332-0012, Japan

ARTICLE INFO

Article history:
Received 7 November 2011
Received in revised form 8 January 2012
Accepted 13 January 2012
Available online 24 January 2012

Keywords:
Solution-exfoliated graphene
Graphene field effect transistor
Graphite-binding peptide
Adsorption

ABSTRACT

The binding affinities of graphite-binding peptides to a graphite surface were electrically characterized using sprayed graphene field effect transistors (SGFETs) fabricated with solution exfoliated graphene. The binding affinities of these peptides were also characterized using atomic force microscopy (AFM) and mechanically exfoliated graphene field effect transistors (GFETs) to confirm the validity of the SGFET platform. Binding constants obtained via GFET and AFM were comparable with those observed using SGFETs. The sprayed graphene film serves as a scalable platform to study biomolecular adsorption to graphitic surfaces.

© 2012 Elsevier B.V. All rights reserved.

1. Introduction

Graphene has been gaining interest as a platform for applications such as biosensors and other bioelectronic devices due to its electrical properties and planar nature (Castro Neto et al., 2009; Novoselov et al., 2004). The formation of stable and uniform functional biomolecular films on graphene is still a limiting factor in the development of practical and effective biosensors. To address this challenge, it is essential to establish means for quantitative characterization of in situ binding affinity and kinetics of biomolecules to graphene. While traditional characterization methods such as surface plasmon resonance (SPR) spectroscopy or quartz crystal microbalance (QCM) come to mind as potential platforms, graphene field effect transistors (GFETs) offer a novel approach for the characterization of molecular adsorption to planar graphitic surfaces via electrical detection (Gong and Yang, 2010; Guo et al., 2010; Hu et al., 2010; Huang et al., 2010; Ohno et al., 2009, 2010). Conventional approaches, however, present practical challenges such as requiring thin, mechanically stable and confluent graphene films on macroscopic sensing elements, e.g. a quartz chip in SPR. GFET-type configurations, on the other hand, require only a continuous electrical pathway to observe in situ adsorption kinetics to an intrinsic graphitic surface. As an alternative to conventional GFETs, pathways of desired length could be produced by using liquid exfoliated graphene (Coleman et al., 2008) in place of the commonly used mechanical exfoliation (Novoselov et al., 2004) or chemical vapor deposition (Reina et al., 2009) methods. Liquid suspended graphene can be sprayed via microdrop printing or other factory-scalable methods to form macroscopic films, which are then used as sensing elements in GFETs. In this work, we demonstrate the sprayed graphene field effect transistor (SGFET) as a scalable sensing platform which electrically monitors the adsorption of biomolecules to an intrinsic graphitic surface.

As a calibration tool to characterize this platform, we use graphite-binding dodecapeptides (GrBPs) recently developed by our group (Oren et al., 2007; So et al., in press). These peptides have a variety of binding affinity values depending on their amino acid sequences, but all interact with the graphene surface non-covalently. One of the graphite binding peptides studied here not only exhibits high coverage and strong binding to graphite, but can also form long-range ordered assembled nanostructures (So et al., in press) possibly because of its amino acid composition and molecular conformation recognizing the graphene surface (Hnilova et al., 2008). This peptide may serve as a robust biomolecular tool for further surface functionalization of the graphitic surfaces.

2. Experimental

2.1. Chemicals and materials

Acetone (#270725, ≥99.9%), Bovine serum albumin (BSA, #A2153 ≥96%), and 1-methyl-2-pyrrolidinone (NMP, #328634 ≥99.5%) were purchased from Sigma–Aldrich. 300 mesh crystalline graphite powder was purchased from Alfa Aesar. Indium pellets (Purity 99.99%) were purchased from Ted Pella. SPI-1 grade highly oriented pyrolitic graphite (HOPG) was purchased from SPI

* Corresponding author. Tel.: +1 206 616 6515.
E-mail address: sarikaya@u.washington.edu (M. Sarikaya).

0956-5663/$ – see front matter © 2012 Elsevier B.V. All rights reserved.
doi:10.1016/j.bios.2012.01.012

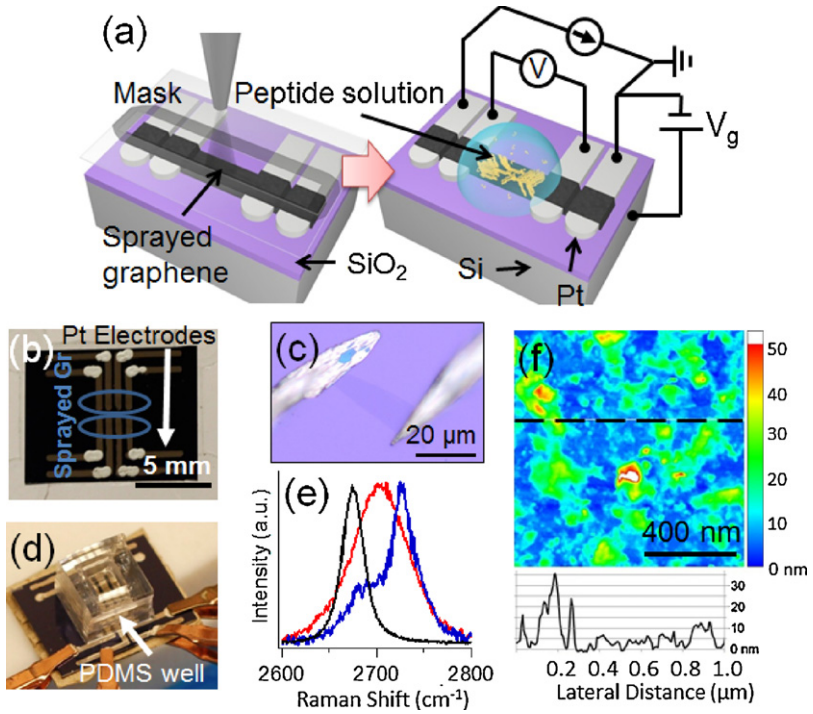

Fig. 1. (a) Schematic of device preparation. Deposit Pt electrodes and spray dispersed graphene solution. After H_2/Ar, anneal, device is ready for exposure to analyte. (b) Image of sprayed graphene field effect transistor (SGFET) substrate. White blots on electrodes are Ag paste for better electrical contact. (c) Image of experimental setup using SGFET substrate. (d) Optical micrograph of graphene field effect transistor (GFET). (e) Raman spectrum of graphene (black), SGFET sensing element (red), and bulk graphite (blue). (f) AFM of sprayed film. Light blue portions denote 2–5 nm multilayer graphene. (For interpretation of the references to color in this figure legend, the reader is referred to the web version of the article.)

supplies. 0.2 μm filters were purchased from Milipore (Milipore Nylon Membrane, 0.20 μm). 100 mm diameter 300 nm oxide layer p-doped Si test wafers were purchased from University Wafers, and cleaved into 21 mm × 16 mm chips. Mechanical masks were fabricated at the University of Washington Mechanical Engineering Machine Shop. Indium microsoldering was done using a Signatone H-100 with a custom resistive heating element. AFM measurements were done using high frequency NanoSensors PPP-NCHR (NanoandMore USA, Lady's Island, SC) noncontact probes with a 42 N/m spring constant.

Two graphite-binding peptide sequences, IMVTESSDYSSY (GrBP5) and TVKCVTKCTTTT (GrBP4) were used in this study. GrBP5 was biocombinatorily selected sequence used previously in literature (So et al., in press), and GrBP4 was bioinformatically designed as a graphite weak binder using a method reported in literature (Oren et al., 2007). Synthesis and preparation of these peptides were done according to methods discussed in previous literature (So et al., 2009).

2.2. Fabrication of SGFET substrate

SGFET sensing substrates were prepared by first sputter coating Ti/Pt (2 nm/50 nm, Gatan Model 682 PECS) electrodes on the silicon substrates through a mechanical mask. This substrate was then heated to ~350 °C using a hotplate, and an exfoliated graphene solution was sprayed on the substrate through another mechanical mask (Fig. 1a). Solution exfoliated graphene was prepared follows: 30 mg of graphite powder was rinsed and sonicated for 5 min with acetone, dried via vacuum filtering with a 0.2 μm filter, sonicated in 30 ml NMP for 1 h, then centrifuged at 4000 rpm (~2000 × *g*, Sorvall RC 5B Plus SLA-1500 rotor) for 8 h. The top 20 ml of exfoliated graphite solution was extracted for spray coating. To eliminate any surface contamination, the prepared substrate was annealed according to literature at 450 °C for 1 h under a flow of 40% H_2, 60% Ar (Ishigami et al., 2007). A completed SGFET substrate is shown in Fig. 1b.

2.3. Fabrication of GFET substrate

Mechanically exfoliated graphene (Novoselov et al., 2004) was used to fabricate conventional GFETs. Indium microsoldering (Girit and Zettl, 2007) was used for electrode deposition in place of lithographic processes to preserve the cleanliness of the graphene surface. An optical micrograph of a completed GFET is shown in Fig. 1c.

2.4. Characterization of sprayed graphene film

The sprayed film was characterized using Raman microscopy (Renishaw Raman Microscope at 514 nm excitation wavelength), and the apparent gate response of the film was probed using an Agilent U2722A USB Modular Source Measure Unit with a current source of 5 μA and a 4-probe setup (simplified circuit diagram in Fig. 1a, right). The topography of the film was observed using a Digital Instruments Multimode AFM under tapping mode.

2.5. Detection of peptide adsorption using SGFET/GFET

The experimental configuration of the SGFET sensing substrate is shown in Fig. 1d, a 4-probe setup with analyte being retained on the surface using a PDMS well. The GFET resistance was monitored using a 2-probe setup with the Agilent U2722A system, also using a PDMS well. The adsorption of two peptides, GrBP4 and GrBP5 was observed using these systems. The adsorption behavior of bovine serum albumin (BSA) was also observed as a positive control, as it is known to produce resistivity change in a similar system (Ohno et al., 2009). Before exposing to peptide solution, each substrate was equilibrated in deionized water for 30 min while monitoring its

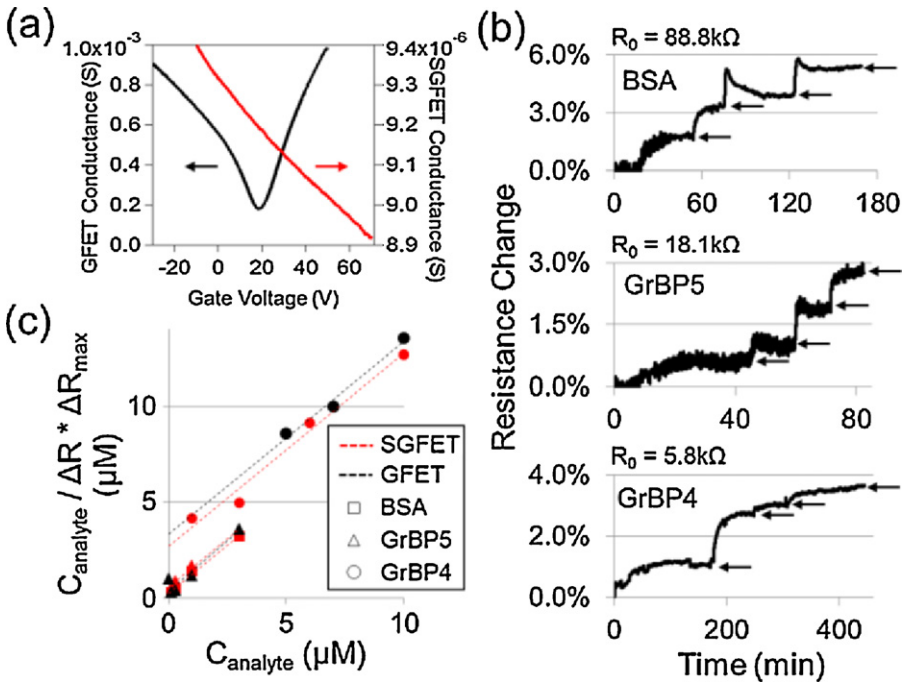

Fig. 2. Data from SGFET and GFET. (a) Gate response of graphene FET device (black, left axis) and SGFET sensing element (red, right axis). (b) Sensograms of adsorption tracked on SGFET. Arrows denote observed equilibrium response levels. (c) Normalized analyte concentration per conductance change ($C_{analyte}/\Delta R \times \Delta R_{max}$) as a function of analyte concentration. The dashed lines are linear fits to the Langmuir adsorption isotherm. Colors indicate sensing platform (black, GFET; red, SGFET), while shapes indicate the analyte (square, BSA; triangle, GrBP5; circle, GrBP4). (For interpretation of the references to color in this figure legend, the reader is referred to the web version of the article.)

resistance. After equilibration, analyte (GrBP5, GrBP4, or BSA) was added in increasing concentrations to bring the total concentration to the desired level. With GrBP5 and BSA, the analyte concentration was increased incrementally from 0.1 μM to 3.0 μM. In the case of GrBP4, the concentrations were increased from 1 μM to 10 μM to allow for reasonable equilibration times.

2.6. Preparation and observation of AFM equilibrium coverage samples

To complement the SGFET results, biomolecular binding affinity was also characterized by atomic force microscopy imaging (AFM) to observe surface coverage of peptides on graphite with various incubation concentrations (0.1 μM to 5 μM). The samples were prepared by mechanically exfoliating graphite flakes on a silicon substrate, incubating these flakes in various concentrations of analyte solutions for 3 h in a humid environmental chamber (>90%), and then blowing the surface with N_2. These samples were immediately imaged using a Digital Instruments Nanoscope-IIIa Multimode AFM under tapping mode, with a scan speed of 5.00 μm/s and target amplitude of 2.00 V.

2.7. Determination of binding constant

Based on the observed resistances at equilibrium, the binding affinity of each peptide was determined using the following form of the Langmuir adsorption isotherm

$$\frac{C_{analyte}}{\Delta R_{ads}} = \frac{1}{\Delta R_{max}} \times C_{analyte} + \frac{1}{\Delta R_{max}} \times \frac{1}{K'_{eq}}$$

where $C_{analyte}$ is the concentration of the analyte solution, ΔR_{ads} is the equilibrium resistance shift observed for a given $C_{analyte}$, ΔR_{max} is the resistance shift at full coverage, and K'_{eq} is the apparent equilibrium constant.[1] Since $C_{analyte}$ and ΔR_{ads} are known from experiment, one can determine ΔR_{max} and K'_{eq} through this formula. As there was no practical method of determining relative surface coverage of adsorbates, ΔR_{max} was used as a normalizing factor to compare between different runs, assuming that all adsorbates would attain full coverage at high enough concentrations. K'_{eq} was determined by multiplying the above equation through by ΔR_{max}, plotting

$$\frac{C_{analyte} \times \Delta R_{max}}{\Delta R_{ads}} = C_{analyte} + \frac{1}{K'_{eq}}$$

and determining the inverse of the *y*-intercept for each data set. Standard error of K'_{eq} was determined through calculating K'_{eq} using equilibrium resistance values ±1 standard deviation from the observed equilibrium resistance for each analyte and testing platform.

3. Results and discussion

3.1. Characteristics of sprayed graphene film

The quality of the sprayed film was characterized using Raman spectroscopy and atomic force microscopy (AFM). Raman spectroscopy can be used to quickly determine the quality of graphene via the 2D band in the spectrum (Ferrari et al., 2006) (Fig. 1e). The Raman peak of our sprayed film is located between the peaks for mechanically exfoliated graphene and bulk graphite. Since the 2D

[1] Though we use the Langmuir model to explore and compare our adsorbates for convenience, it is important to note that the value we arrive at is not strictly a Langmuir equilibrium constant. Because BSA and peptides are not expected to bind reversibly to the graphene surface, we cannot follow the Langmuir assumptions, so it would be misleading to refer to the comparison factor as K_{eq}. Therefore, we adopt K'_{eq} as our factor for comparing relative adsorption strengths between the adsorbate and the graphene, which we refer to as the "apparent equilibrium constant".

peak in our spectrum does not have the characteristic shoulder seen in 5+ layer graphite, we assume the dominant flake thickness is approximately 2–4 graphene layers. AFM images of the film show the thickness ranged approximately from 0 to 50 nm, with regions of ~5 nm (blue to light blue in Fig. 1f) and thicker 10–30 nm regions (turquoise to light green on Fig. 1f). Though the conductive film as a whole is a composite of aggregated graphene and few-layer graphene flakes, enough portions along the conductive path are of few-layer graphene for these regions to dominate the electrical resistivity across the film and allow the observance of a gate response, as will be seen below.

The gate response of the SGFET and GFET were observed. Fig. 2a shows the gate response for a GFET (black) and our sprayed graphene film (red). Although much shallower than that of the GFET, the sprayed film exhibited sensitivity to an applied gate voltage, allowing it to detect a resistance change due to surface adsorption.

3.2. Adsorption detection with SGFET

GrBP and BSA adsorption was observed using our SGFET platform. Contrary to previous literature on GFETs (Ohno et al., 2009), the resistivity increased as analyte concentration was increased, and equilibrium was usually reached within an hour (Fig. 2b). The difference in resistance shift between our results and those observed in literature most likely stems from tracking conductance at different sides of the charge-neutral point (CNP). Ohno et al. tracked device conductance using $V_{tg} = -0.1$ V ($V_{tg} <$ CNP) and observed an increase in conductance, indicating a positive shift in the CNP or a decrease of carrier mobility (see Fig. S4 for graphical representation using an arbitrary IV_{tg} profile). If one were to track device conductance at $V_{tg} >$ CNP, it would decrease from the same IV_{tg} profile response to BSA adsorption. Although we currently cannot confirm this hypothesis since due to the lack of a reference electrode to probe our devices' IV_{tg} profiles, we plan to include the addition of a reference electrode to the list of future improvements to the system in order to allow the elucidation of this phenomenon.

The apparent equilibrium constants obtained from these studies were $0.8 \pm 0.3\ \mu M^{-1}$ for GrBP5, $0.4 \pm 0.1\ \mu M^{-1}$ for GrBP4, and $3.6 \pm 0.2\ \mu M^{-1}$ for BSA (Table S1). These results support our original selection in GrBP5 being a stronger graphite binder than GrBP4, but we also observe that it is a weaker binder than the non-specifically adsorbing and more massive BSA.

Reproducibility was quantitatively assessed through four repeats of GrBP5 adsorption with good correlation (Fig. S1). Our devices displayed a stable signal when exposed to deionized water, as well as deionized water under a flow rate of 80 μl/min., a flow rate comparable to molecular adsorption characterization tools such as SPR. Our platform's response appears approximately linear, with good correlation between signal vs. coverage (Fig. 3b), particularly for GrBP4, but there are slight discrepancies in the device linearity when detecting GrBP5 and BSA adsorption, of which are discussed further in the Supplemental Materials. The sensitivity of our platform was higher than that of conventional GFET biomolecular sensors when compared per device, but was far lower when the sensor surface area was taken into account. A detailed discussion of the SGFET platform's reproducibility, stability, linear range, and sensitivity are included in the Supplemental Materials (Figs. S1–S3).

3.3. Adsorption detection with GFET

Adsorption of GrBP5 was also observed using GFETs to confirm the measurements obtained by our sprayed graphene sensing platform under the same aqueous conditions. Again, contrary to the previous literature (Ohno et al., 2009), the resistivity increased as analyte concentration was increased. The apparent equilibrium

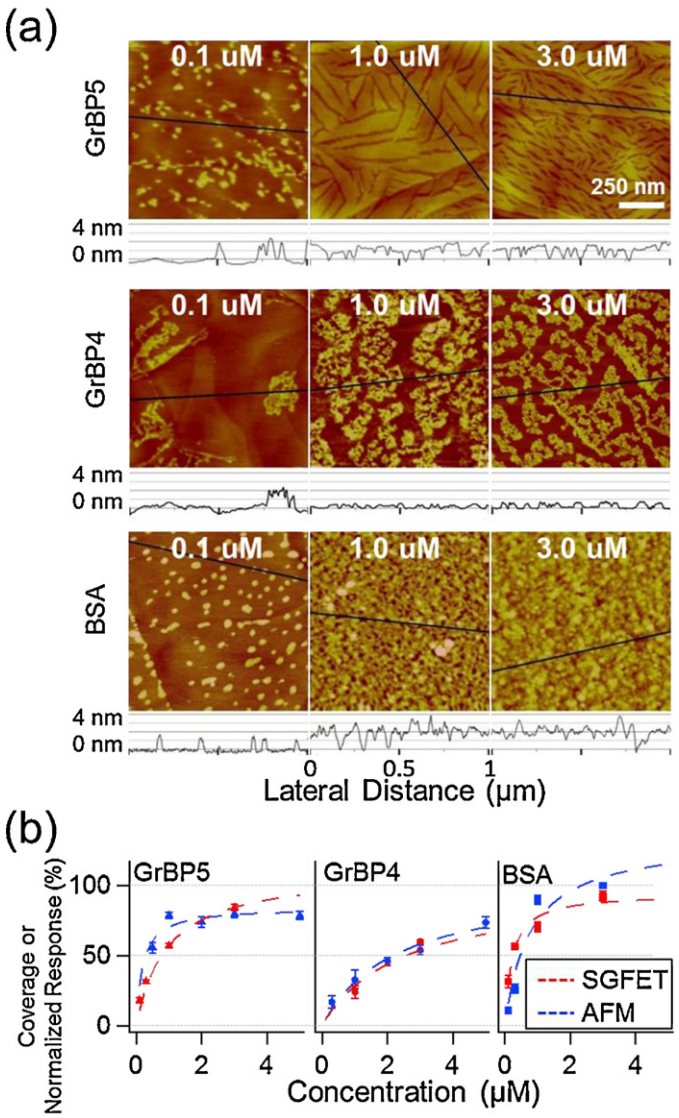

Fig. 3. Comparison of AFM data with SGFET data. (a) AFM images of surface morphology on HOPG at equilibrium for each concentration. (b) Langmuir isotherm fits of equilibrium coverage in SRS and AFM.

constants obtained through GFET adsorption measurements were $5.4 \pm 2.1\ \mu M^{-1}$ for GrBP5 and $0.3 \pm 0.1\ \mu M^{-1}$ for GrBP4 (Table S1). These values illustrated good agreement with the SGFET values. The equilibrium results from GFET and the sprayed graphene sensor were plotted in Fig. 2c, showing good agreement between the two adsorption characterization techniques. Since the affinity of the peptides to mechanically exfoliated graphene was similar to that on the in-solution exfoliated graphene, it can be concluded that our sprayed graphene sensor acts similarly to GFET, regardless of our platform's larger number of interconnections and edges. These results also suggest that our sprayed graphene substrates are clean enough to obtain a clear adsorption signal, much like a mechanically exfoliated GFETs.

3.4. Adsorption detection with AFM

Fig. 3a shows representative AFM images of various concentrations of each analyte, and Fig. 3b compares the actual coverage obtained through AFM to the normalized response obtained through SGFET. Each measurement is close to that obtained with the novel platform, with the most discrepancy being from BSA. A

potential source of discrepancy can be seen in the line profile of the 1.0 μM and 3.0 μM BSA samples: these profiles show the partial formation of adlayers (4 nm thick regions, as opposed to the discrete 2 nm features observed at low concentration). Coverage in an AFM study is only recognized as the regions of graphite that are occupied by analyte molecules, and does not take adlayer molecules into account. In SGFET, adlayer molecules may contribute to the doping of the sprayed graphene layer, resulting in a higher-than-expected "full coverage" value. This difference in detection may be responsible for the higher discrepancy between AFM and SGFET for BSA adsorption, particularly as adlayer formation is not observed for GrBP4 or GrBP5. However, the AFM results still confirm the relative K'_{eq}s of the peptides obtained with the other two sensing platforms, with apparent binding constants of 2.23 μM^{-1} for GrBP5, 0.49 μM^{-1} for GrBP4, and 1.21 μM^{-1} for BSA (Table S1).

4. Conclusions

In conclusion, the binding characteristics of the peptides obtained using this platform were consistent with that obtained using two other platforms: AFM coverage analysis and GFET sensors, confirming the viability of the novel platform. The experiments carried out using the SGFET platform should also be possible using other single-layer materials such as MoS_2 and WS_2 through the preparation of the respective single-layer solutions discussed in previous literature (Coleman et al., 2011).

The experiments in this study were carried out with peptides in deionized water and with no counter electrode in order to simulate the conditions used in the initial selection of the peptides. To better control environmental conditions such as surface potential, electrochemical systems typically employ reference and counter electrodes, and a buffer to stabilize solution conditions. Further studies should investigate these factors to establish more stable measurement of molecular adsorption. Under a better-controlled environment, kinetic constants of biomolecular adsorption such as deposition rate and sticking coefficient can also be evaluated (Jung and Campbell, 2000).

The GrBPs examined here are part of a molecular toolset called genetically engineered peptides for inorganics (GEPIs) (Sarikaya et al., 2003). This toolset offers a host of peptides which selectively bind to a wide variety of different materials (metals, oxides, minerals, etc.), a number of which have been used in literature as a viable platform for the immobilization of functional proteins to solid surfaces (Demir et al., 2011; Sarikaya et al., 2009; Tamerler et al., 2009). The expansion of this toolset to graphitic surfaces, with possibilities to other single-layer materials, opens up new possibilities of quantitative functionalization of multi-material substrates.

Acknowledgments

We thank Hilal Yazici and Candan Tamerler for the bio-combinatorial selection of the strong graphite-binding peptide (GrBP5), Emre E. Oren for the bioinformatic selection of the weak graphite-binding peptide (GrBP4), Carolyn Gresswell for peptide synthesis, and Brandon Wilson for discussions on SPR and QCM. This research was supported by NSF-Biomaterials (DMR-0706655) and MRSEC program (DMR-0520567) at GEMSEC, Genetically Engineered Materials Science and Engineering Center, University of Washington. C.S. and Y.H. were supported by the NCI Training Grant T32CA138312 (NIH) and JST PRESTO programs (Japan), respectively, and also by NSF Biomat program. T.R.P. and M.S. were supported by MRSEC. The work was carried out at the GEMSEC-SECF, a member of Materials Facilities Network of MRSEC.

Appendix A. Supplementary data

Supplementary data associated with this article can be found, in the online version, at doi:10.1016/j.bios.2012.01.012.

References

Castro Neto, A.H., Guinea, F., Peres, N.M.R., Novoselov, K.S., Geim, A.K., 2009. Rev. Mod. Phys. 81 (1), 109–162.
Coleman, J.N., Hernandez, Y., Nicolosi, V., Lotya, M., Blighe, F.M., Sun, Z.Y., De, S., McGovern, I.T., Holland, B., Byrne, M., Gun'ko, Y.K., Boland, J.J., Niraj, P., Duesberg, G., Krishnamurthy, S., Goodhue, R., Hutchison, J., Scardaci, V., Ferrari, A.C., 2008. Nat. Nanotechnol. 3 (9), 563–568.
Coleman, J.N., Lotya, M., O'Neill, A., Bergin, S.D., King, P.J., Khan, U., Young, K., Gaucher, A., De, S., Smith, R.J., Shvets, I.V., Arora, S.K., Stanton, G., Kim, H.Y., Lee, K., Kim, G.T., Duesberg, G.S., Hallam, T., Boland, J.J., Wang, J.J., Donegan, J.F., Grunlan, J.C., Moriarty, G., Shmeliov, A., Nicholls, R.J., Perkins, J.M., Grieveson, E.M., Theuwissen, K., McComb, D.W., Nellist, P.D., Nicolosi, V., 2011. Science 331 (6017), 568–571.
Demir, H.V., Seker, U.O.S., Zengin, G., Mutlugun, E., Sari, E., Tamerler, C., Sarikaya, M., 2011. ACS Nano 5 (4), 2735–2741.
Ferrari, A.C., Meyer, J.C., Scardaci, V., Casiraghi, C., Lazzeri, M., Mauri, F., Piscanec, S., Jiang, D., Novoselov, K.S., Roth, S., Geim, A.K., 2006. Phys. Rev. Lett. 97 (18.).
Girit, C.O., Zettl, A., 2007. Appl. Phys. Lett. 91 (19.).
Gong, S.Q., Yang, M.H., 2010. Chem. Commun. 46 (31), 5796–5798.
Guo, Y.J., Guo, S.J., Ren, J.T., Zhai, Y.M., Dong, S.J., Wang, E.K., 2010. ACS Nano 4 (9), 5512.
Hnilova, M., Oren, E.E., Seker, U.O., Wilson, B.R., Collino, S., Evans, J.S., Tamerler, C., Sarikaya, M., 2008. Langmuir 24 (21), 12440–12445.
Hu, P.A., Zhang, J., Li, L., Wang, Z.L., O'Neill, W., Estrela, P., 2010. Sensors 10 (5), 5133–5159.
Huang, Y.X., Dong, X.C., Shi, Y.M., Li, C.M., Li, L.J., Chen, P., 2010. Nanoscale 2 (8), 1485–1488.
Ishigami, M., Chen, J.H., Cullen, W.G., Fuhrer, M.S., Williams, E.D., 2007. Nano Lett. 7 (6), 1643–1648.
Jung, L.S., Campbell, C.T., 2000. Phys. Rev. Lett. 84 (22), 5164–5167.
Novoselov, K.S., Geim, A.K., Morozov, S.V., Jiang, D., Zhang, Y., Dubonos IV, S.V., Firsov, G.A.A., 2004. Science 306 (5696), 666–669.
Ohno, Y., Maehashi, K., Matsumoto, K., 2010. Biosens. Bioelectron. 26 (4), 1727–1730.
Ohno, Y., Maehashi, K., Yamashiro, Y., Matsumoto, K., 2009. Nano Lett. 9 (9), 3318–3322.
Oren, E.E., Tamerler, C., Sahin, D., Hnilova, M., Seker, U.O.S., Sarikaya, M., Samudrala, R., 2007. Bioinformatics 23 (21), 2816–2822.
Reina, A., Jia, X.T., Ho, J., Nezich, D., Son, H.B., Bulovic, V., Dresselhaus, M.S., Kong, J., 2009. Nano Lett. 9 (1), 30–35.
Sarikaya, M., Kacar, T., Ray, J., Gungormus, M., Oren, E.E., Tamerler, C., 2009. Adv. Mater. 21 (3), 295–299.
Sarikaya, M., Tamerler, C., Jen, A.K.Y., Schulten, K., Baneyx, F., 2003. Nat. Mater. 2 (9), 577–585.
So, C.R., Hayamizu, Y., Yazici, H., Gresswell, C., Khatayevich, D., Tamerler, C., Sarikaya, M., doi:10.1021/nn204631x, in press.
So, C.R., Kulp, J.L., Oren, E.E., Zareie, H., Tamerler, C., Evans, J.S., Sarikaya, M., 2009. ACS Nano 3 (6), 1525–1531.
Tamerler, C., Kacar, T., Zin, M.T., So, C., Wilson, B., Ma, H., Gul-Karaguler, N., Jen, A.K.Y., Sarikaya, M., 2009. Biotechnol. Bioeng. 103 (4), 696–705.